Observation of spatial modulation instability in intracavity second-harmonic generation

A. V. Mamaev,* P. Lodahl,† and M. Saffman

Department of Physics, University of Wisconsin, 1150 University Avenue, Madison, Wisconsin 53706

Received June 17, 2002

We report the observation of spatial instabilities in singly resonant intracavity second-harmonic generation. Self-focusing as well as spatially ordered near- and far-field structures are observed. Experimental results are compared with mean-field analysis as well as three-dimensional numerical simulations. © 2003 Optical Society of America

OCIS codes: 190.0190, 190.4420.

Spatial instabilities and interactions of beams in media with quadratic nonlinearity have been studied intensely in recent years. Research in this area is motivated by applications to all-optical switching and image processing[1–3] as well as interest in quantum optical aspects of spatial structures[4–8] for use in low-noise imaging and precision measurements.[9–11] A single pass of sufficiently intense radiation through a nonlinear crystal can result in focusing and (or) defocusing effects that lead to soliton formation as well as convective modulational instability and multisoliton generation.[12,13] Alternatively, an intracavity geometry can be used that provides feedback for the incident and (or) generated beams. The intracavity geometry has been predicted to lead to absolute modulational instabilities, spatial patterns, and solitons in both parametric oscillation and second-harmonic generation (SHG) configurations.[14–19] Evidence for structure formation in parametric oscillation in a stable resonator was reported in Ref. 20.

We describe here the results of a SHG experiment in a cavity with planar mirrors pumped by a wide Gaussian-type beam. The use of a planar resonator allows us to make direct contact with the large body of theoretical work devoted to this configuration. We concentrate on parameters where a possible internally pumped parametric oscillation does not strongly influence the transverse structure formation.[19] The experimental results are consistent with the presence of an absolute instability that is due to the presence of cavity feedback. We note that the intracavity modulational instability reported here is observed with pump intensities that are orders of magnitude lower than those that one would need to observe instabilities in propagation experiments.[12,13] Numerical simulations of mean-field and cavity models based on three-dimensional propagation equations result in structures and spatial scales similar to those observed experimentally.

The experimental arrangement shown in Fig. 1 uses an $L_c = 10$ mm long by 3×3 mm wide a-cut $KNbO_3$ crystal with antireflection coating ($R < 0.5\%$) at 860/430 nm on one end and a high-reflection coating ($T < 0.5\%$) at 860/430 nm on the other end. The dichroic mirror placed between the input coupler and the crystal has a reflectivity of 99% at 860 nm and a transmission of 95% at 430 nm. Thus a high-finesse linear resonator with planar mirrors is formed by the high-reflection end of the crystal and the input coupler. The generated second harmonic escapes from the cavity after passing through the dichroic mirror. We can vary the distance L_{air} between the antireflection end of the crystal and the input coupler from 1.5 to 10 mm to change the length of the cavity.

To generate the pump radiation we start with a continuous-wave beam of ~100 mW at 860 nm from a single-longitudinal-mode ring Ti:sapphire laser. The 860-nm radiation is passed through a 2-cm-long Ti:sapphire rod five times and pumped with 100-mJ pulses from a doubled Nd:YAG laser. The resulting infrared pulses have a peak power of up to 20 kW in a 150-ns-long (FWHM) pulse. The 150-ns pulse corresponds to ~690 SHG cavity round trips when $L_{\mathrm{air}} = 1$ cm.

The ratio of the internal circulating power to the external pump power is given by the cavity buildup factor $B = T[1 - \sqrt{(1 - T)R_L}\,]^{-2}$, where T is the intensity transmission coefficient of the input coupler, R_L is the effective round-trip cavity reflectivity in the presence of internal losses, and we have neglected any nonlinear loss resulting from SHG. We estimate the internal reflectivity as $R_L = 1 - 2(0.01 + 0.005 + 0.03) - 0.005 = 0.905$, where the numerical factors from left to right represent the dichroic mirror, the crystal antireflection coating, the crystal internal loss, and the crystal high-reflection coating. With a $T = 5\%$ input coupler we get a cavity finesse of 43, a HWHM linewidth of

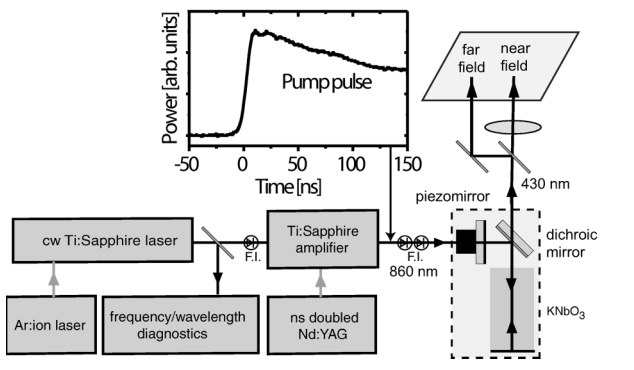

Fig. 1. Experimental setup: F.I.'s, Faraday isolators; ns, nanosecond. The inset shows a typical temporal profile of the pump pulse.

0146-9592/03/010031-03$15.00/0

$\gamma/2\pi = 62$ MHz, and a projected buildup factor of $B \simeq 10$. The buildup deduced from measurements of the transmission in an aligned and misaligned cavity (experimental ratio ≤ 150) was $B_{\mathrm{exp}} \sim 8$. We attribute the reduction in B_{exp} compared with the value predicted from loss measurements to be due to our use of wide beams, which amplifies the deleterious effects of scattering and crystal inhomogeneities.

For pump powers below the instability threshold, the fundamental and second-harmonic fields in the cavity are smooth, Gaussian-type beams. For higher powers spatial structures are observed, as shown in Fig. 2 for a pump beam diameter of $d \sim 500$ μm (FWHM) and peak power of $\sim$10 kW. The crystal temperature is adjusted for $\Delta k L_c \sim 3$, which gives an effective self-focusing nonlinearity,[19] and the cavity phase is adjusted close to resonance. The cavity tuning is characterized below, by use of the normalized detuning $\Delta = (\omega - \omega_c)/\gamma$, where ω is the pump laser frequency and ω_c is the frequency of the nearest cavity mode. Although hexagonal symmetry is seen in the far field, the near field has only three bright spots on the off-axis ring. For our experimental parameters with $L_{\mathrm{air}} = 4$ mm, mean-field theory[19] predicts a spatial scale of $\sim$1.2 mm, which is too large compared with the pump beam diameter to yield a fully developed hexagon in the near field. Reduction of the symmetry class and compression of the spatial scale when a focused pump beam was used have also been seen in Kerr-type media.[21] Inhomogeneities in the crystal available at present prevented us from using a larger beam.

We can compare the experimental pump power needed for observation of spatial instability with the analytical prediction of mean-field theory. The results of mean-field plane-wave analysis[19] for $\Delta k L_c \sim 3$ are shown in Fig. 3. For this value of phase mismatch, plane-wave cavity bistability does not coexist with the transverse instability that is present for $\Delta \gtrsim -2.2$.[22] We see that the instability threshold has a minimum for $\Delta \sim -1$ and increases approximately quadratically with increasing detuning. At the optimum detuning the theoretical threshold power calculated with the experimental beam diameter is $\sim$140 W. The transverse wave number has the normal diffractive scaling as the square root of the detuning: $k_\perp \sim \sqrt{\Delta + \Delta_{\mathrm{NL}}}$, where Δ_{NL}, which is positive for $\Delta k L_c \sim 3$, is the nonlinear part of the detuning. Although the absolute value of the cavity detuning was not stabilized, the sharp theoretical minimum in the threshold power suggests that the observed structures were obtained at small negative detunings close to the minimum of the threshold. This is consistent with the observation from a large number of shots that the measured transverse wave number varied by less than 30%, although we also expect the limited pump beam size to suppress variations in the transverse scale. Note also that for $\Delta \gtrsim -0.2$ the threshold for internally pumped parametric oscillation is lower than the transverse instability threshold, and the former may coexist with transverse structures, although the parametric beams were not observed in this work. While the parametric oscillation can have a strong influence on the temporal stability of the cavity mode,[23] theoretical studies of both singly[19] and doubly[24] resonant SHG show that the parametric beams strongly suppress structure formation for positive detuning of the fundamental. This suggests, together with the pump threshold and spatial wave-number data, that the observed structures were obtained for small negative values of the cavity detuning. Pattern formation for negative cavity detuning is a unique feature of SHG for which the total cavity detuning can be written as the sum of a linear and a nonlinear part, in contrast with the optical parametric oscillator, for which $k_\perp \sim \sqrt{\Delta}$ so that there is no transverse instability for negative detuning.

We see that the pump intensity at the threshold of modulational instability predicted by mean-field theory for a plane-wave pump is as much as 50 times lower than the experimental value needed with a focused pump beam because of the spatial scale compression. The observed pump power requirements can be verified by simulations of the cavity dynamics with a focused pump beam. The bottom row in Fig. 2 was obtained by numerical solution of the paraxial propagation equations [Eqs. (25) and (26) in Ref. 19]

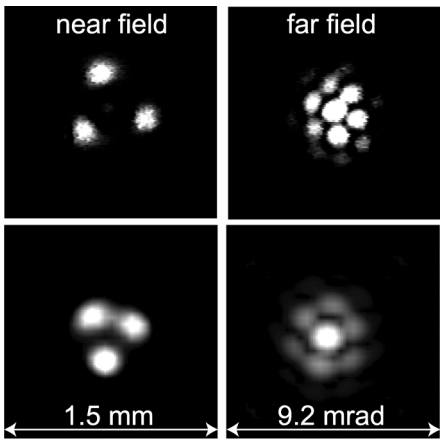

Fig. 2. Transverse structures in the second-harmonic beam. Top row, experiment; bottom row, numerical simulation.

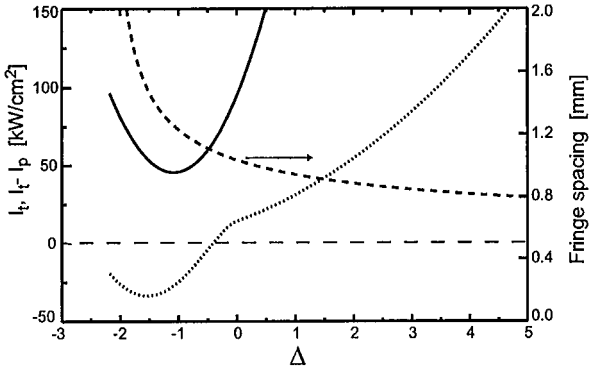

Fig. 3. Mean-field calculation of pump beam intensity I_t at threshold (solid curve), difference of the transverse threshold and the threshold for internally pumped parametric oscillation $I_t - I_p$ (dotted curve), and pattern fringe spacing (dashed curve) as a function of normalized cavity detuning Δ for $\Delta k L_c = 3$.

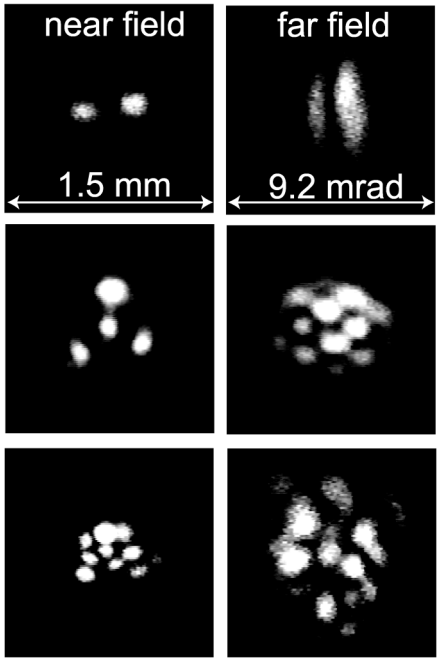

Fig. 4. Experimental pictures of spatial structures in the second harmonic observed with increasing pump powers of approximately 1, 5, and 20 kW from top to bottom.

over a time corresponding to 230 cavity round trips. Parameter values in a range of ±25% relative to the experimental ones gave numerical results similar to those shown in Fig. 2. As the pump intensity was increased, a bifurcation sequence of near-field structures was observed, ranging from single-spot self-focusing to two spots, four spots, five spots, a hexagonal structure, and unstable random filamentation. Inclusion of ~10% pump beam ellipticity, which was present experimentally, resulted in the three spot patterns shown in Fig. 2 for a pump power of ~2 kW. With the assumption of $\Delta \sim -1$, the spatial and angular scales observed in experiment and numerics agree to within ~30%. Even with a spatially limited beam the intracavity geometry allows instabilities to be observed with pump intensities that remain 3 orders of magnitude lower than those used in single-pass experiments without a cavity.[13] We note that structures similar to those seen in Fig. 2 can also be obtained from single-pass experiments with sufficiently large nonlinearity.[25] However, the agreement between numerics and experiment indicates that the observed structures are not the result of a convective instability but rather are spatially compressed versions of the patterns predicted in the presence of optical feedback.[19]

For larger and smaller pump beam widths and powers, different structures were seen both in simulations and in the experiment, as shown in Fig. 4. These included self-focusing to a single spot and to different numbers of near-field spots. Similar structures were also seen in the fundamental beam. At the highest pump powers of ~20 kW, random distributions of bright self-focused filaments were observed, as shown in the bottom row of Fig. 4.

In conclusion, we have observed spatial modulational instabilities in a quadratically nonlinear cavity with spatial and angular scales that are in agreement with numerical simulations.

This work was supported by National Science Foundation grant 0200372 and by the European Science Foundation PHASE network. M. Saffman (e-mail: msaffman@facstaff.wisc.edu.) is an A. P. Sloan Foundation fellow.

*Permanent address, Institute for Problems in Mechanics, Russian Academy of Sciences, Prospekt Vernadskogo 101, Moscow, 117526 Russia.

†Present address, Faculty of Applied Physics, University of Twente, P.O. Box 217, 7500 AE Enschede, The Netherlands.

References

1. B. Costantini, C. De Angelis, A. Barthelemy, B. Bourliaguet, and V. Kermene, Opt. Lett. **23,** 424 (1998).
2. S. Minardi, G. Molina-Terriza, P. Di Trapani, J. P. Torres, and L. Torner, Opt. Lett. **26,** 1004 (2001).
3. A. Bramati, W. Chinaglia, S. Minardi, and P. Di Trapani, Opt. Lett. **26,** 1409 (2001).
4. M. I. Kolobov, Rev. Mod. Phys. **71,** 1539 (1999).
5. A. Gatti and L. Lugiato, Phys. Rev. A **52,** 1675 (1995).
6. E. M. Nagasako, R. W. Boyd, and G. S. Agarwal, Phys. Rev. A **55,** 1412 (1997).
7. P. Lodahl and M. Saffman, Opt. Lett. **27,** 110 (2002).
8. P. Lodahl and M. Saffman, Opt. Lett. **27,** 551 (2002), erratum of Ref. 7.
9. S.-K. Choi, M. Vasilyev, and P. Kumar, Phys. Rev. Lett. **83,** 1938 (1999).
10. S.-K. Choi, M. Vasilyev, and P. Kumar, Phys. Rev. Lett. **84,** 1361 (2000), erratum of Ref. 9.
11. C. Fabre, J. B. Fouet, and A. Maître, Opt. Lett. **25,** 76 (2000).
12. W. E. Torruellas, Z. Wang, D. J. Hagan, E. W. Van Stryland, G. I. Stegeman, L. Torner, and C. R. Menyuk, Phys. Rev. Lett. **74,** 5036 (1995).
13. R. A. Fuerst, D.-M. Baboiu, B. Lawrence, W. E. Torruellas, G. I. Stegeman, S. Trillo, and S. Wabnitz, Phys. Rev. Lett. **78,** 2756 (1997).
14. G.-L. Oppo, M. Brambilla, and L. A. Lugiato, Phys. Rev. A **49,** 2028 (1994).
15. K. Staliunas, J. Mod. Opt. **42,** 1261 (1995).
16. S. Trillo and M. Haelterman, Opt. Lett. **21,** 1114 (1996).
17. C. Etrich, U. Peschel, and F. Lederer, Phys. Rev. Lett. **79,** 2454 (1997).
18. S. Longhi, Phys. Rev. A **53,** 4488 (1996).
19. P. Lodahl and M. Saffman, Phys. Rev. A **60,** 3251 (1999).
20. M. Vaupel, A. Maître, and C. Fabre, Phys. Rev. Lett. **83,** 5278 (1999).
21. T. Ackemann and W. Lange, Phys. Rev. A **50,** R4468 (1994).
22. P. Lodahl and M. Saffman, Opt. Commun. **184,** 493 (2000).
23. M. Bache, P. Lodahl, A. V. Mamaev, M. Marcus, and M. Saffman, Phys. Rev. A **65,** 033811 (2002).
24. P. Lodahl, M. Bache, and M. Saffman, Opt. Lett. **25,** 654 (2000).
25. R. S. Bennink, V. Wong, A. M. Marino, D. L. Aronstein, R. W. Boyd, C. R. Stroud, Jr., S. Lukishova, and D. J. Gauthier, Phys. Rev. Lett. **88,** 113901 (2002).